EAI Endorsed Transactions
on Energy Web
Research Article EAI.EU

Study on the Economic and Technical Optimization of Hybrid Rural Microgrids Integrating Wind, Solar, Biogas, and Energy Storage with AC/DC Conversion

Hu Tan[1,a], Xiaoliang Wang[1,b], Tingting Xu[1,c], Ke Zhao[1,d], Lianchao Su[1,e], Wenyu Zhang[1,f], Zheng Xin[2,*,g]

[1]State Grid Shandong Electric Power Company, Weifang Power Supply Company, Weifang, 261021, Shandong, China
[2]Shandong Jianzhu University, School of Information and Electrical Engineering, Jinan, 250101, Shandong, China

Abstract

Under the guidance of the 'dual carbon' goals and 'rural revitalization' strategy, the development of microgrids primarily based on wind, solar, and biogas energy is rapidly advancing in rural areas. A critical and challenging area of current research is how to optimally configure the capacity of these microgrids of varying sizes, taking into account the availability of resources in the system's environment and specific climatic conditions, to maximize economic benefits. Based on this, the article constructs a model of a hybrid AC/DC microgrid system powered by wind, solar, and biogas energy. It undertakes multi-objective optimization to achieve the highest utilization of renewable energy, the most economical cost, and the minimum carbon emissions while ensuring the reliability of the system's power supply. The study explores the economically and technically optimal configuration of this microgrid energy system under certain climatic conditions. The results indicate that the optimal configuration for a rural microgrid powered by wind, solar, and biogas energy should include a 2.6 kW biogas generator, 30.00 kW solar panels, 5.24 kW wind turbines, a 2.6 kW battery storage system, and a 10.00 kW bidirectional inverter. This configuration results in the lowest total net cost of the system, achieving optimal outcomes in terms of total net cost, cost per kilowatt-hour, and supply reliability.

Keywords: Electricity Market; Multi-Energy Complementary System, Rural Microgrid; Integration of Generation, Grid, Load, and Storage, Economic and Technical Analysis

Received on 15 November 2023, accepted on 10 April 2024, published on 16 April 2024

doi: 10.4108/ew.5803

1. Introduction1

China aims to reach its carbon peak by 2030 and achieve carbon neutrality by 2060. Agricultural greenhouse gas emissions account for 7%-8% of the country's total emissions, and energy use in agricultural production and daily life contributes to about 15% of the national total. To actively promote the rural revitalization strategy in line with the 'dual carbon' goals, rural microgrids have become a research focus in recent years. The off-grid independent operation of rural microgrids has the advantages of environmental friendliness, flexible operation, and high reliability. It can meet the end-users' requirements for power quality, supply reliability, and safety. Simultaneously, it can address the difficulties in supplying power to remote areas and reduce reliance on traditional fossil fuels. However, distributed generation (DG) facilities, particularly those relying on renewable sources like wind and solar, are heavily influenced by environmental factors, exhibiting significant fluctuations. The intermittent and fluctuating nature of wind and solar-based distributed generation complicates the distribution of power flows when integrated on a large scale into the grid. This complexity and difficulty in prediction result in challenges in the scheduling of the distribution network.

The integration of distributed generation disrupts the characteristics of traditional passive radial networks in the power distribution system. The unidirectional power flow

[a]tanhu8621950@sina.com, [b]706415299@qq.com, [c]nydiaxt@sina.com, [d]304778726@qq.com, [e]wssg878@sina.com, [f] 562371532@qq.com, [*g]Corresponding author. Email: xinzheng9309@163.com

and voltage drop characteristics of traditional radiative networks no longer exist, leading to deteriorated voltage distribution in the power grid. This introduces new distribution characteristics in the operation indicators of the distribution network, posing significant challenges to its safe operation. To meet the daily load demands of users and alleviate the impact of distributed generation on the safe and stable operation of the distribution network, careful consideration must be given to the capacity configuration and equipment selection of distributed energy sources.

Economic and technical optimization of distributed generation equipment is mainly influenced by local climatic conditions. Deng [1] established a model for wind/solar/storage/diesel microgrid power source configuration, aiming to minimize annual system costs and optimize the model using an improved Grey Wolf Optimization algorithm. Tan et al. [2,3] focused on the capacity configuration of distributed power sources in wind/solar/diesel/storage independent hybrid microgrids, considering various constraints. They integrated system reliability, economy, environmental friendliness, and energy efficiency indicators to construct a multi-objective optimization model, exploring improved optimal operation control strategies. YU et al. [4-6] built an isolated wind/solar/hydrogen/storage DC microgrid output model, establishing a capacity optimization model with the lowest power shortage rate and lowest cost per unit of electricity as objectives, and optimized it using the MOBASDE algorithm. CHENG [7] established an independent solar/hydro/diesel/storage microgrid, considering economic, environmentally friendly, and supply reliability aspects. They developed different optimization models with various objectives and obtained optimal solutions for capacity allocation, focusing on analyzing differences and reasons between various capacity optimization designs but not analyzing changes in storage capacity. YANG et al. [8-10] built an independent hydro/solar/diesel/storage microgrid, considering economic, environmental benefits, and supply reliability. They proposed a multi-objective optimization model for microgrid power source capacity and used the Particle Swarm Optimization algorithm under certain control strategies for model solving. However, diesel generators have a lower proportion in rural areas compared to biogas. NI et al.[11-13] analyzed typical daily loads in isolated microgrid conditions and optimized the capacity of photovoltaic batteries and energy storage sources, but it focused on a single optimization objective without proposing specific solution methods. YAO et al. [14] considering the reliability of wind/solar/storage independent microgrids and renewable energy waste, aimed to optimize the levelized cost of energy (LCOE) using the Monte Carlo Simulation embedded in the Gravitational Search Algorithm (GSA-MCS) for model solving. LI et al. [15,16] used HOMER software to build different models, determining the most economical solutions based on net present cost (NPC), LCOE, initial cost, operating cost, and lowest total cost through simulation and optimization.

Previous articles approached the issue of power source capacity configuration from the perspectives of optimizing intelligent algorithms or constructing and improving multi-objective functions, but the model construction and solving process were complex. This paper opts to build an off-grid rural residential wind/solar/biogas/storage microgrid model in the end-user area. Focusing on the capacity configuration of distributed power sources and considering various constraints, it integrates the system's economic and reliability indicators. The paper aims to optimize the net present cost over the system's entire lifecycle, including reliability economic penalties, using HOMER general planning software for system model solving. It compares the economic indicators of a single energy source supply system with the optimally configured system to analyze the system's economic benefits.

2. Structure of Wind-Solar-Biogas Storage Rural Microgrid

The schematic diagram of the off-grid residential wind-solar-biogas storage microgrid studied in this paper is shown in Figure 1. The system consists of a wind turbine, photovoltaic panels, a biogas mixed-fuel generator, batteries, and converters. The wind turbine and photovoltaic panels can convert renewable energy sources such as wind and solar energy into electrical energy. This energy is then converted into alternating current by the converters to meet the daily load demand of users. The charging and discharging process of the battery can facilitate power trading with the grid, addressing the randomness and instability issues of wind and solar power, thus enhancing the quality of electricity and the reliability of the system. The biogas fuel generator can serve as a backup power source, ensuring normal electricity usage for users when renewable energy generation devices cannot meet the load demand.

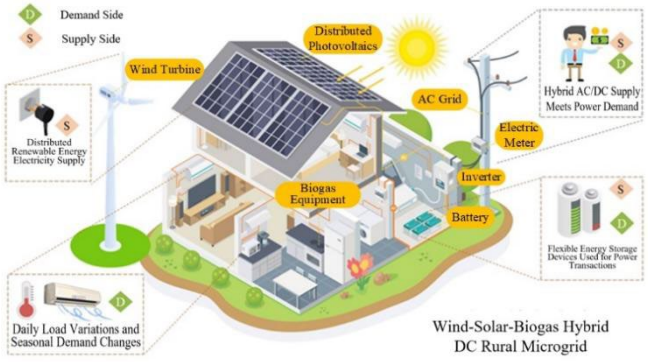

Figure 1. Structure diagram of house type microgrid with wind-solar-biogas-battery

3. Wind-Solar-Biogas Storage System

3.1 Mixed Fuel Generator Model

The hybrid fuel generator selects and simultaneously burns two types of fuels, diesel and biogas, with the corresponding model as follows.

(a) Diesel Generator Model

The diesel generator uses diesel as its power source, and there is a linear relationship between its output power and fuel consumption, as shown in Eq.1.

$$Fuel = \alpha_1 P_R + \alpha_2 P_0 \quad (1)$$

Where: $Fuel$- Diesel generator fuel consumption, α_1- Intercept coefficient of the fuel consumption curve for the diesel generator, measured in L/hr/kW, α_2- Slope of the fuel consumption curve, measured in L/hr/kW, P_R - Rated power of the diesel generator, P_0- Actual power output of the diesel generator in kW.

The system generator has a minimum load ratio (output) requirement set at 20% of the rated power.

(b) Biogas Power Generation Model

In the biomass biogas power generation model, it is assumed that biogas power generation is strongly correlated with pressure, biogas consumption, and power, as shown in Eq.2.

$$P_G = b_1 + b_2 G_P + b_3 G_V + b_4 G_P^2 \quad (2)$$

Where: P_G- Output power of biogas power generation, G_P- Biogas pressure, G_V- Biogas consumption, b_1- Constant term coefficient, b_2, b_3- Linear coefficients of biogas power generation with respect to biogas pressure and consumption, b_4 is a constant coefficient.

3.2 Photovoltaic Power Generation Model

The photovoltaic output power is influenced by factors such as irradiance intensity, the surface temperature of the photovoltaic panel, and others. Its output power is given by Eq.3.

$$P_{PV}(t) = P_{STC} \frac{L_{WC}(t)}{L_{STC}} \{1 + k[T_{WC}(t) - T_{STC}]\} \quad (3)$$

Where: $P_{PV}(t)$- Actual output power of the photovoltaic panel at time t, P_{STC}- Rated output power of the photovoltaic panel under standard conditions, $L_{WC}(t)$ - Irradiance intensity under working conditions, i.e., kW/m2, L_{STC} - Irradiance intensity under standard conditions, k - Temperature coefficient, $T_{WC}(t)$- Surface temperature of the photovoltaic panel at time t under working conditions, T_{STC}- Surface temperature of the photovoltaic panel under standard conditions.

3.3 Wind Turbine Generator Model

The real-time output power of the wind turbine generator unit is a linear function of the wind speed. The specific expression for the power generation model is as Eq.4.

$$P_{WT}(v) = \begin{cases} 0 & 0 \le v(t) \le v_i \\ P_r \frac{v(t)-v_i}{v_r - v_i} & v_i \le v(t) \le v_r \\ P_r & v_r \le v(t) \le v_0 \\ 0 & v(t) \ge v_0 \end{cases} \quad (4)$$

Where: $P_{WT}(v)$ - Output power of the wind turbine generator, P_r- Rated power of the wind turbine generator, $v(t)$- Real-time wind speed, v_i- Cut-in wind speed of the wind turbine generator, v_r- Rated wind speed, v_0- Cut-out wind speed.

3.4 Battery Model

In this article, we select the lead-acid storage battery (Trojan L16P) as the energy storage component of the system. The battery operates in two states during its operation, charging and discharging. Its mathematical operating model is as Eq.5-6.

a. Charging State

$$P_{bat}(t) = P_{bat}(t-1) + \left[P_s(t) - \frac{P_c(t)}{\eta_n}\right]\eta_c \quad (5)$$

b. Discharging State

$$P_{bat}(t) = P_{bat}(t-1) - \left[\frac{P_c(t)}{\eta_n} - P_s(t)\right]/\eta_d \quad (6)$$

Where: $P_{bat}(t)$- The amount of electricity stored in the battery at time t, $P_s(t)$- The sum of the output power from distributed sources at time t, $P_c(t)$- The sum of the total load demand at time t, η_n- Inverter conversion efficiency, η_c- Battery charging efficiency, η_d - Battery discharging efficiency.

An important parameter for the battery during its usage is the State of Charge (SOC), which represents the percentage of the remaining capacity of the battery compared to its rated capacity. SOC varies during the charging and discharging processes and is defined as Eq.7-8.

a. During the charging process

$$SOC(t) = SOC(t-1) + \frac{P_{bat}\eta_c T}{E_{bat}} \quad (7)$$

b. During the discharging process

$$SOC(t) = SOC(t-1) + \frac{P_{bat} T}{\eta_d E_{bat}} \quad (8)$$

Where: $SOC(t)$- the state of charge of the battery at time t, P_{bat}- the operating power of the battery, E_{bat}- the rated capacity of the battery; η_c- the charging efficiency of the battery, η_d- the discharging efficiency of the battery, T- sampling time.

4. Independent Microgrid Optimization Configuration Model

4.1 System Optimization Objectives

While ensuring power supply reliability and meeting load demands, the pursuit of economic operation and guaranteeing investment benefits is essential. Therefore, within the system constructed in this paper and subject to relevant conditional constraints, the total net present cost (TNPC) over the system's entire lifecycle is established as the economic indicator for optimization purposes, forming the objective function.

TNPC

TNPC of the system is the present value of all costs incurred by the system over its lifetime minus the present value of all revenues generated by the system during its lifetime. Since the system being discussed in this article is an off-grid independent operation microgrid, without grid connection, costs associated with purchasing electricity from the grid and revenues from grid sales are not considered. The distributed energy sources in the system are all clean energy, and the system is established in suburban areas at the urban periphery, exempting it from emission fines. Therefore, the total net present value of this system only considers the capital costs, replacement costs, operation and maintenance (O&M) costs, fuel costs, and residual income of each component, as shown in Eq.9-10.

$$C_{TNPC} = C_{TC} + C_{TR} + C_{TO\&M} + C_{TF} + C_{TS} \tag{9}$$

Where: C_{TNPC}- Total Net Present Cost of the system, C_{TC} - Total Capital Cost of the system, C_{TR} - Total Replacement Cost of the system, $C_{TO\&M}$ - Total Operation and Maintenance Cost of the system, C_{TF} - Fuel Cost of the system; C_{TS} - Total Residual Value of the system.

$$\begin{cases} C_{CT} = C_G + C_{WT} + C_{PV} + C_{bat} + C_{ct} \\ C_{TR} = C_G^R + C_{WT}^R + C_{PV}^R + C_{bat}^R + C_{ct}^R \\ C_{TO\&M} = C_G^{O\&M} + C_{WT}^{O\&M} + C_{PV}^{O\&M} + C_{bat}^{O\&M} + C_{ct}^{O\&M} \\ C_{TF} = C_G^{fuel} \\ C_{TS} = C_G^{sal} + C_{WT}^{sal} + C_{PV}^{sal} + C_{bat}^{sal} + C_{ct}^{sal} \end{cases} \tag{10}$$

Where: $C_G, C_{WT}, C_{PV}, C_{bat}, C_{ct}$ - Initial investment costs of the hybrid fuel generator, wind turbine, photovoltaic panel, battery, and inverter; C_G^R, C_{WT}^R, C_{PV}^R, C_{bat}^R, C_{ct}^R - Replacement costs of the hybrid fuel generator, wind turbine, photovoltaic panel, battery, and inverter; $C_G^{O\&M}$, $C_{WT}^{O\&M}$, $C_{PV}^{O\&M}$, $C_{bat}^{O\&M}$, $C_{ct}^{O\&M}$ - Operating and maintenance costs of the generator, wind turbine, photovoltaic panel, battery, and inverter; C_G^{fuel} - Fuel costs of the generator; C_G^{sal}, C_{WT}^{sal}, C_{PV}^{sal}, C_{bat}^{sal}, C_{ct}^{sal} - Residual values of the generator, wind turbine, photovoltaic panel, battery, and inverter, all component residual values are negative in the calculation of the total net present value of the system.

New Energy Utilization Rate

New Energy Utilization Rate is a quantifiable indicator of a system's capacity to integrate new energy sources. It represents the ratio of the total electrical energy generated by the new energy components within the electrical system to the total electrical load of the system. To ensure efficient utilization of new energy sources, the new energy utilization rate is considered as an optimization objective within the system. The expression for the new energy utilization rate is as shown in Eq.11.

$$f_{new} = 1 - \frac{P_{nonnew}}{P_{load}} \tag{11}$$

Where: P_{nonnew} - Generation capacity of non-new energy components; P_{load} - Total load of the electrical system.

4.2 Constraints

The Constraints are as shown in Eq.12.

$$\begin{cases} P_L(t) + P_{exc}(t) = P_G(t) + P_{PV}(t) + \\ \quad P_{WT}(t) + P_{bat}(t) + P_{def}(t) \\ P_{i,min} \le P_i \le P_{i,max} \\ SOC_{min} \le \mathrm{SOC}(t) \le SOC_{max} \\ f_{LPSP} \le f_{LPSP,max} \end{cases} \tag{12}$$

Where: $P_L(t)$ - Actual power of the load; $P_{exc}(t)$ - Power; $P_G(t)$, $P_{PV}(t)$, $P_{WT}(t)$, $P_{bat}(t)$ - Output power of the generator, photovoltaic, wind turbine, battery; $P_{def}(t)$ - Non-essential load; $P_i, P_{i,min}, P_{i,max}$ - Actual output power, minimum output power, maximum output power of the nth power source; $f_{LPSP,max}$ - Maximum permissible power shortage probability of the system; f_{LPSP} - Probability that the system cannot meet load demand within a given time, with a time duration of the entire year comprising 8760 hours, as shown in Eq.13.

$$f_{LPSP} = \frac{\sum_{i=1}^{8760}[P_L(t_i) - P_S(t_i)]}{\sum_{i=1}^{8760} P_L(t_i)} \tag{13}$$

Where: $P_S(t_i)$ - The sum of the output power from all sources in the system.

4.3 Optimization function

In this paper, ensuring power supply reliability forms the foundation. The total net cost of the system, i.e., the lifetime costs, is the fundamental optimizing variable. In the optimization model development process, reliability constraints, such as capacity shortages, are transformed into penalties, classified under additional O&M costs, and amalgamated with the system's fixed O&M costs into a unified O&M cost category within the objective function, as shown in Eq.14-15.

$$C_{cs} = c_{cs} \cdot P_{cs} \tag{14}$$

$$P_{cs} = \sum_{i=1}^{8760}[P_L(t_i) - P_S(t_i)] \tag{15}$$

Where: c_{cs} - Penalty for capacity shortage, in yuan per kWh; P_{cs} - Total deficient capacity, in kWh per year.

The final optimization objective function is denoted as F, in Eq.16.

$$F = Min(C_{TNPC} + C_{cs} + \frac{\lambda}{f_{new}}) \tag{16}$$

Where: λ - The coefficient of the constant term.

4.4 Multi-objective Particle Swarm Optimization algorithm

Using Multi-Objective Particle Swarm Optimization (MOPSO) to optimize the wind-solar-biogas storage system. MOPSO is an optimization algorithm that considers multiple objective functions simultaneously and identifies their Pareto optimal solution sets. In optimizing the wind-solar-biogas storage system, there are multiple objective functions to consider, such as maximizing energy storage and minimizing costs. MOPSO helps identify the Pareto optimal solution sets between these objectives, achieving the best balance between maximizing energy storage and minimizing costs within the storage system. The MOPSO algorithm utilizes particle positions and velocities to explore the solution space of the problem. Each particle represents a potential solution and is updated based on its current position and velocity. Through iterative updates to their positions and velocities, particles gradually converge towards the Pareto optimal solution set. When using MOPSO, the objective functions and constraints are as described earlier.

The algorithm includes the following steps:

Initialize the positions and velocities of the particle swarm.

Compute the fitness value for each particle.

Update the velocity and position of each particle based on its current best fitness value and the swarm's best fitness value.

If the stopping condition is met (e.g., maximum iteration reached), stop iterating; otherwise, return to step 2.

5. Case study analysis

5.1 Meteorological Conditions Description

Weifang region in Shandong province was chosen as the study area. The Weifang area has a warm temperate continental monsoon climate with distinct seasons, abundant sunlight, and prevalent winds in both summer and winter. The rural areas are extensive, making it suitable for the selection of distributed generation. The typical DC and AC power load demands of local users are illustrated in Figure 2.

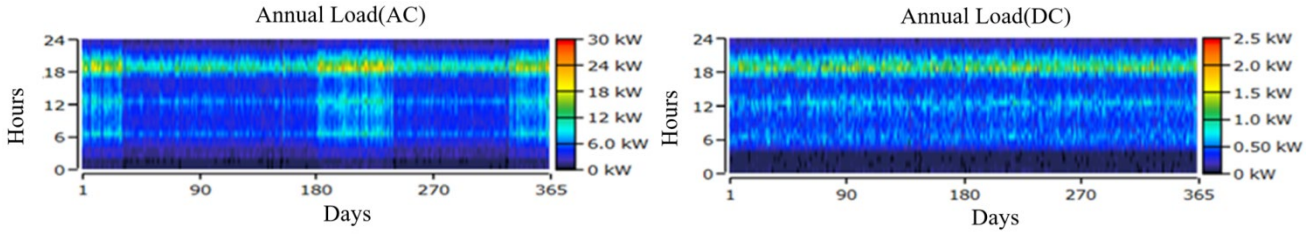

Figure 2. Annual load chart for rural areas (AC/DC)

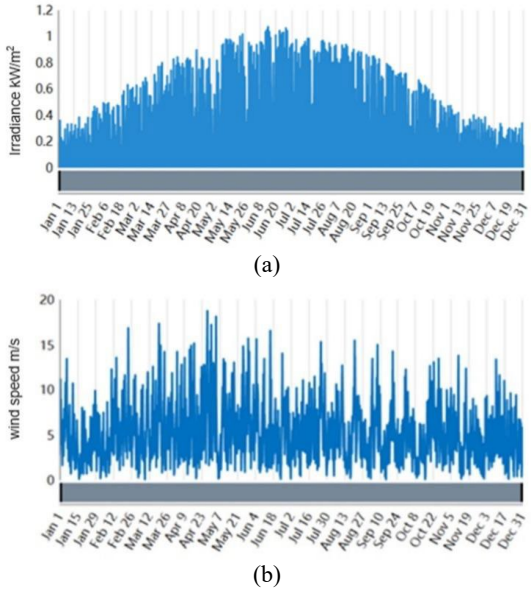

Figure 3. Annual meteorological data in Weifang areas (a) radiations; (b) wind speed; (c) temperture

Annual monthly average meteorological data such as wind speed, sunlight, and temperature for the selected area within the National Renewable Energy Laboratory are chosen. In the simulation process, utilizing the Weibull

distribution, discrete annual data for wind speed, sunlight, and temperature are derived, as depicted in Figure 3.

The meteorological conditions in the specific region and the end-user load demands should determine the optimal configuration scheme. For the microgrid equipment, various component-related price parameters and energy parameters are shown in Table 1. Typical seasonal purchase cost of electric energy in Weifang area are shown in Figure 4.

Table 1. Relevant parameters of system components

Equipment	Biogas	Wind turbine	Photovoltaic	Battery	Inverter Rated
Capacity/kW	2.60	1.24	5.00	1.30	-
Investment Cost/yuan	5706	31700	22190	1902	4755
Replacement Cost/yuan	5706	31700	22190	1902	4755
O&M Cost/yuan·kW-1·year	84.4	511.3	63.4	63.4	-
Lifespan/years	5.7	20	25	10	15

Set the system's lifecycle at 25 years, maximum annual shortage probability at 2%, nominal discount rate at 8%, real discount rate at 5.88%, expected inflation rate at 2%. Sequentially input resource data for each component, simulation time step of 60 minutes, and perform simulation on the selected case study.

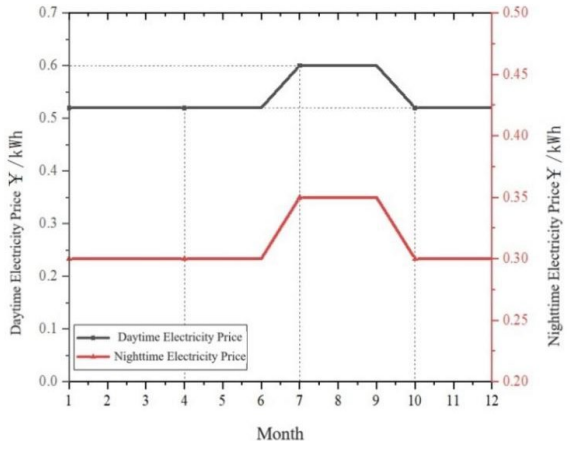

Figure 4. Typical seasonal purchase cost of electric energy in Weifang area

5.2 Simulation Results and Analysis

Based on the aforementioned parameters, evaluate the economic and technical feasibility of different technical solutions, considering variations in technical costs and energy availability. Arrange the simulation results in ascending order of the system's total net cost for each scenario. Additionally, categorize and summarize the different combinations of output sources. The optimized configuration schemes used are presented in Table 2.

Table 2. Optimal configuration scheme of partial system capacity

Scenario	Dual-fuel generator /kW	Wind turbine/kW	Photovoltaic/kW	Battery /pieces	Inverter /kW	Total Net Present Cost of the System / ¥ 10k	Capacity Shortage Probability /%
1	2.6	5	10.00	2	10.00	13.01	0
2	2.6	10	20.00	4	10.00	13.80	0
3	2.6	15	30.00	6	10.00	14.85	0
4	2.6	20	20.00	8	10.00	14.86	0
5	2.6	25	30.00	10	10.00	19.21	2

Analyzing the simulation results, the economic indicators of the five optimized configurations are presented in Figure 5. From Figure 5, the following observations can be made: 1) Comparing Scenario 1 with Scenarios 2, 3, 4, and 5 reveals a significant increase in initial system costs, unit generation costs, and total net cost after incorporating wind and photovoltaic power. This is attributed to the instability of wind and solar power, leading to a substantial increase in battery capacity and subsequently higher battery costs. Consequently, the economic benefits generated by the system are lower, resulting in increased total net cost and unit generation cost. 2) Comparing Scenarios 1, 2, 3, 4, and 5 demonstrates that when the system utilizes both renewable energy sources and co-fired generators for power generation, the total net cost and unit generation cost are lower compared to systems solely reliant on either renewable energy or co-fired generators. The utilization of two renewable energy sources complements each other, enhancing energy utilization efficiency and reducing costs. However, systems relying solely on renewable energy sources have higher initial investment costs, while co-fired generators incur higher operating costs due to their higher fuel expenses. 3) In comparison to Scenarios 2, 3, 4, and 5, Scenario 1 respectively saves 5.67%, 12.37%, 12.42%, and 32.24% in total costs and reduces unit generation costs by 5.50%, 12.17%, 12.37%, and 33.15%. This demonstrates the effectiveness of the coupled system.

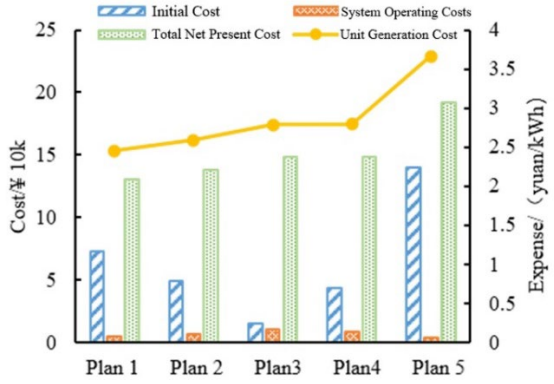

Figure 5. Economic index data of configuration scheme

From Figure 6, it's evident that in Scenarios 1, 2, 3, and 4, the microgrid system's electricity generation can adequately meet the users' base load demand. Within the system, the co-fired generator functions as a backup power source. In cases where the other power sources are running at full capacity and still cannot meet the load demand, the co-fired generator supplements the system to ensure power supply reliability. In Scenario 5, solely relying on renewable energy for power generation leads to a significant increase in electricity generation. However, due to its instability, the utilization rate for power generation is lower, resulting in an increased likelihood of capacity shortage within the system.

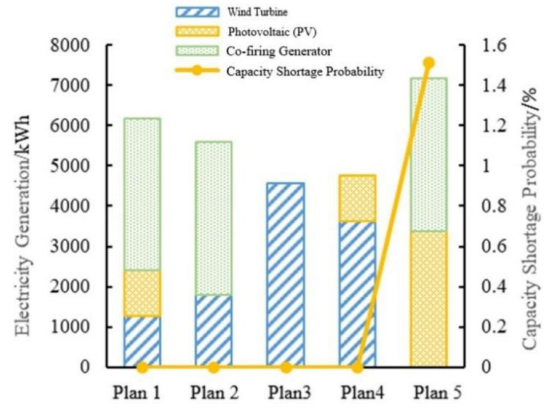

Figure 6. Power generation and capacity shortage probability data of configuration scheme

The optimal configuration derived from the analysis of the results is as follows: a 2.6 kW capacity for the fuel generator, a 10.00 kW capacity for the photovoltaic panel, a 5 kW capacity for the wind turbine, two batteries of 1.3 kW each, and a bidirectional inverter with a capacity of 10.00 kW. The total net cost of the system amounts to 130,100 yuan, representing the lowest total net cost among all configurations and achieving the best balance among various evaluation indicators. Considering the energy availability and system economics of the selected research area, solar energy, wind energy, and biogas are recommended as energy sources for electricity generation. Sole reliance on photovoltaic or wind power in the system is not recommended as it would increase the system's investment cost and reduce its economic efficiency.

The cash flow of each component contributing to the total net cost of the system for the aforementioned configuration is illustrated in Figure 7. From the graph, it's apparent that initial costs, replacement, and fuel constitute the three major expenses of the total net cost. Initial costs represent the largest proportion at 51.98%, with 79.07% of this portion allocated to the initial investments in the photovoltaic panel and wind turbine. Replacement costs follow, accounting for 20.78%, with 84.26% of these costs incurred in the replacement of the wind turbine and batteries throughout the system's lifecycle, making it another significant expenditure within the total net cost. Fuel costs also constitute a substantial portion of the total net cost, mainly due to the high price of diesel fuel, which is included in the production cost of biogas fuel.

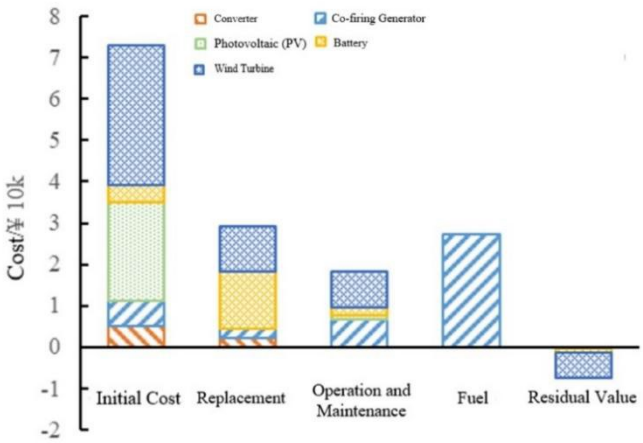

Figure 7. Summary of system cash flow by expense type

When conducting the simulation, the baseline system chosen was reliant on traditional power generation methods, specifically using only a fuel generator as the system's base configuration. The optimal configuration, the winning solution, was compared economically with the chosen baseline scenario to analyze the economic impact of integrating renewable energy generation components into the system. The comparative results are presented in Table 3.

5.3 Multi-Objective Optimization Results

Upon defining the objective function and constraints: Firstly, it's essential to establish the objective function and constraints for optimization. For the wind-solar-biogas

storage system, constraints might include limitations on storage device capacity and minimizing dependence on the power grid. The algorithm commences by randomly initializing the position and velocity of each particle. Compute the fitness value for each particle: Utilize the defined fitness function to compute the fitness value for each particle. Update the velocity and position of each particle based on its current best fitness value and the swarm's best fitness value. The resulting Pareto optimal solution parameters are presented in Table 3. The optimal parameters comprise a 2.6 kW biogas equipment, a 30.00 kW photovoltaic panel, a 5.24 kW wind turbine, a 2.6 kW battery set, and a bidirectional inverter with a capacity of 10.00 kW. The multi-objective optimization and Pareto optimal results are depicted in Figure 8.

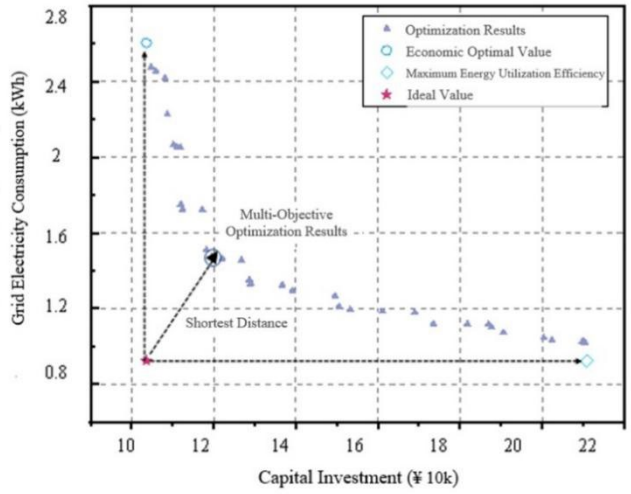

Figure 8. Multi-objects optimization and Pareto optimization

Table 3. Economic comparison between optimal allocation scheme and basic scheme

Plan	Basic Plan	Optimal Configuration Plan
Total Net Present Cost (NPC) / ¥ 10k	16.80	13.01
Initial Cost / ¥ 10k	0.61	7.30
Unit Electricity Generation Cost /yuan·kWh^{-1}	3.16	2.45

Compared to the basic plan, the internal rate of return (IRR) of the project based on the optimal configuration plan is 15%, with a simple payback period of 5.9 years. Simultaneously, as indicated in Figure 9, due to higher initial component investments, the cash outflow of the optimal configuration plan is higher than that of the basic plan for approximately the first 4 years of the system lifecycle. Furthermore, throughout the entire system lifecycle, the cash outflow of the optimal configuration plan remains lower than that of the basic plan, with a positive time coefficient between the two.

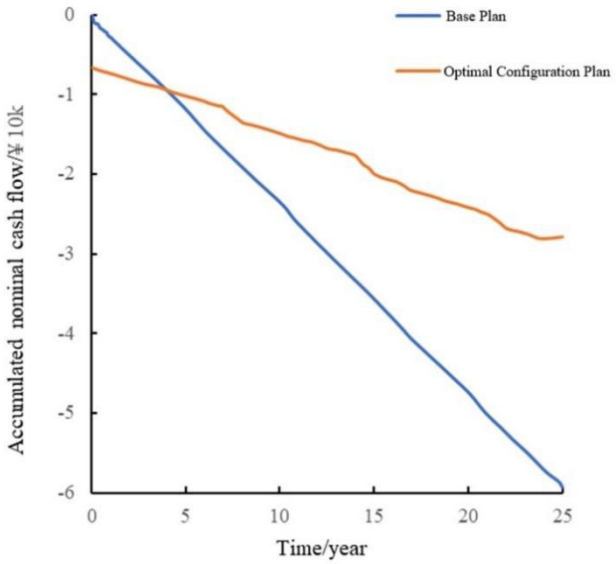

Figure 9. Cumulative nominal cash flow data in the system life cycle

It is evident that, while ensuring the reliability of power supply and meeting load demands, adopting renewable energy in the form of distributed generation shows a more pronounced economic advantage over traditional power generation methods. This approach achieves comprehensive benefits in power generation, environmental conservation, and economics, making it more suitable for rural microgrids. As depicted in Figure 10, greenhouse gases also reveal that the highest system energy efficiency doesn't necessarily equate to economic optimization. Instead, economic optimization is primarily associated with carbon emissions from biogas, posing the greatest environmental impact. Hence, optimal energy sourcing can significantly minimize environmental damage and reduce carbon emissions to the maximum extent possible, while also maximizing the efficient utilization of energy equipment.

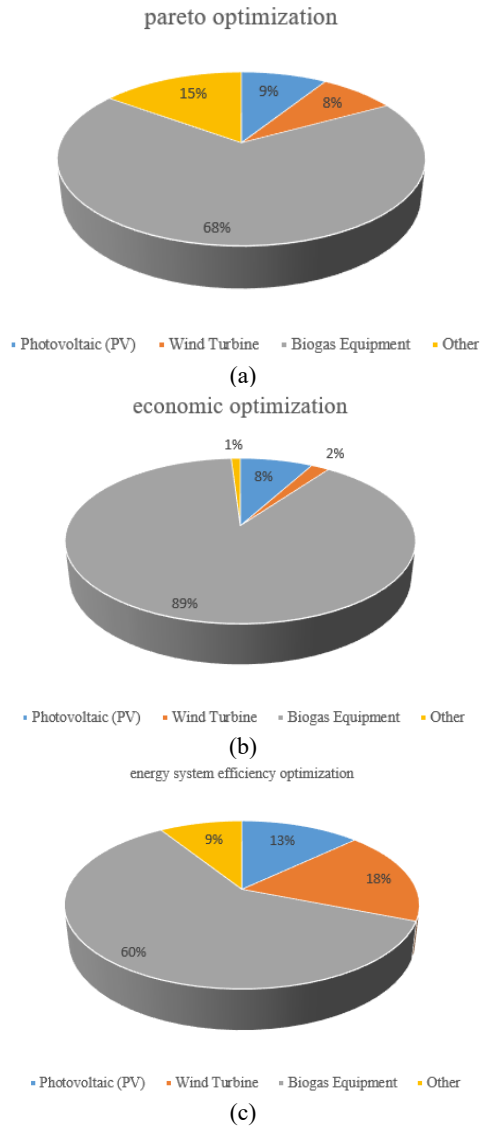

Figure 10. Greenhouse gas emissions over system life cycle (a) pareto optimization (b) economic optimization (c) energy system efficiency optimization

6. Conclusion

This paper has constructed a small-scale microgrid hybrid energy system incorporating wind, solar, and biogas storage. While ensuring power supply reliability and stability, it proposes an optimal configuration model under specific climatic conditions. The specific innovations are as follows:

A comprehensive optimization model for system reliability and economic costs was developed for the wind-solar-biogas storage microgrid system, considering regional meteorological data. This effectively reduces economic costs and enhances equipment utilization.

Under specific climatic conditions, the optimal configuration consists of: a 2.6kW capacity for the fuel generator, 30.00kW for photovoltaic panels, 5.24kW for wind turbines, 2.6kW for battery packs, and a bidirectional inverter capacity of 10.00kW, with a total net present cost of 130,100 RMB. Costs are reduced by at least 5.67% compared to other configurations.

Compared to the base plan, the internal rate of return (IRR) for the project based on the optimized configuration, obtained through multi-objective optimization, is 17%, with a simple payback period of only 5.9 years. The economic advantages are evident, ensuring a comprehensive benefit of secure, reliable, economically and environmentally beneficial power supply.

The proposed wind-solar-biogas hybrid DC microgrid for rural areas is beneficial for optimizing renewable energy utilization and grid load balancing. It promotes the efficient use of clean renewable energy, expands the rural renewable energy market, drives energy structural transformation, and accelerates the achievement of 'dual carbon' goals and rural revitalization.

Acknowledgements

This work was supported by State Grid Shandong Power supply company Project “Research on Multi type Energy Storage Collaborative Optimization and Control Technology for Agricultural Comprehensive Energy System with Full Consumption of Distributed New Energy” (Grant No. 520604220004), and National Key Research and Development Program of China (Grant No. 2022YFB2402900).

References

[1] ZHAO, C., WANG, B., et al. (2022). OPTIMAL CONFIGURATION OPTIMIZATION OF ISLANDED MICROGRID USING IMPROVED GREY WOLF OPTIMIZER ALGORITHM. Acta Energiae Solaris Sinica. 43(01), 256-262.

[2] TAN, Y., LV, Z. L, LI, J. (2016). Multi-objective optimal sizing method for distributed power of wind-solar-diesel-battery independent microgrid based on improved electromagnetism-like mechanism. Pwer System Protection and Control. 44(08), 63-70.

[3] WANG, X. Y., TANG, Z., PU, R. Q. (2019). Optimal Configuration for Stand-alone Microgrid Capacity Based on Improved Operation Control Strategy. Water Resources and Power. 37(04), 192-196.

[4] YU, K. X., LI, F. X., LI, S. S. (2021). Simulation of Multi-Objective Capacity Optimization Configuration of Isolated Microgrid Based on Improved BASDE Algorithm. Power System and Clean Energy. 37(08), 109-117.

[5] Sharma, K. K., Gupta, A., Kumar, R., Chohan, J. S., Sharma, S., Singh, J., & Dwivedi, S. P. (2021). Economic evaluation of a hybrid renewable energy system (HRES) using hybrid optimization model for electric renewable (HOMER) software—a case study of rural India. International Journal of Low-Carbon Technologies, 16(3), 814-821.

[6] Ma, L., Gao, S., Li, M., Pei, Y., & Cheng, S. (2023). Evolutionary multi-objective optimization algorithms in microgrid power dispatching. Frontiers in Energy Research, 10, 1053325.

[7] CHENG R, Feng LI, CHANG Y.(2019). Power capacity optimization design of standalone microgrid. Distributed Energy Resources,4(3), 8-15.

[8] YANG, Q., YUAN, Y., et al. Optimal capacity configuration of standalone hydro-photovoltaic-storage microgrid. Electric Power Automation Equipment. 35(10), 37-44.
[9] Ali, S. A., Mohd R. A., et al.(2020). Feasibility analysis of grid-connected and islanded operation of a solar PV microgrid system: A case study of Iraq. Energy, 191(C).
[10] CHENG, R., CHANG, Y., HUANG, H., et al. (2017). Multi-objective Based Optimal Capacity Design of Isolated Microgrid. Distributed Energy Resources, 35(10), 198-202.
[11] NI, W. B., KANG, K., et al. Optimization of Capacity Configuration for Island Microgrids. Telecom Power Technology. 37(12), 16-18.
[12] Xu, Y., Wu, L., Walker, S. L., Lian, J., Verma, A., & Zhang, R. (2021). Guest editorial: Multi-energy microgrid: Modelling, operation, planning, and energy trading. Energy Conversion and Economics, 2(3), 119-121.
[13] Mekonnen, T., Bhandari, R., & Ramayya, V. (2021). Modeling, analysis and optimization of grid-integrated and islanded solar PV systems for the Ethiopian residential sector: Considering an emerging utility tariff plan for 2021 and beyond. Energies, 14(11), 3360.
[14] Qingcheng, Y. A. O., & Xiaoling, Y. U. A. N. (2020). Optimal configuration of independent microgrid based on Monte Carlo processing of source and load uncertainty. Energy Storage Science and Technology, 9(1), 186.
[15] Li, X., Gao, J., You, S., Zheng, Y., Zhang, Y., Du, Q., & Qin, Y. (2022). Optimal design and techno-economic analysis of renewable-based multi-carrier energy systems for industries: A case study of a food factory in China. Energy, 244, 123174.
[16] Yang, L., Hu, Z., Xie, S., Kong, S., & Lin, W. (2019). Adjustable virtual inertia control of supercapacitors in PV-based AC microgrid cluster. Electric Power Systems Research, 173, 71-85.